Electrochemical stability of organic electrolytes in supercapacitors: Spectroscopy and gas analysis of decomposition products

P. Kurzweil*, M. Chwistek

University of Applied Sciences, Kaiser-Wilhelm-Ring 23, D-92224 Amberg, Germany

Available online 2 September 2007

Abstract

The fundamental aging mechanisms in double-layer capacitors based on alkylammonium electrolytes in acetonitrile were clarified for the first time. After abusive testing at cell voltages above 4 V, ultracapacitors cast out a crystalline mass of residual electrolyte, organic acids, acetamide, aromatics, and polymer compounds. The mixture could be reproduced by electrolysis. The decomposition products of active carbon electrodes and electrolyte solution after a heat treatment at 70 °C were identified by infrared and ultraviolet spectroscopy, liquid and headspace GC–MS, thermogravimetric analysis, and X-ray diffraction. The alkylammonium cation is destroyed by the elimination of ethene. The fluoroborate anion works as source of fluoride and hydrogenfluoride, and boric acid derivates. Acetonitrile forms acetamide, acetic and fluoroacetic acid, and derivates thereof. Due to the catalytic activity of the electrode, heterocyclic compounds are generated in the liquid phase. The etched aluminium support under the active carbon layer is locally destroyed by fluorination. Exploring novel electrolytes, ionic liquids were characterized by impedance spectroscopy.

© 2007 Elsevier B.V. All rights reserved.

1. Introduction

After more than one and a half decade of development, double-layer capacitors are hesitantly going to conquer the markets of energy storage systems, wind mills, and hybrid vehicles [1,2]. Literature about the aging mechanisms in so-called supercapacitors or ultracapacitors is scarce all the same [3–6]. The parasitic chemical reactions at the phase boundary of active carbon electrodes and organic electrolytes have widely been nebulous so far. In long-time experiments, the cases of commercial supercapacitors swell visibly. The equivalent series resistance

increases by a factor of 1.5–5 during 1000 h of operation at rated voltage (2.5 V) and ambient temperatures between 70 and 90 °C [3]. The decrease of capacitance by about 10% is far less affected by heat.

Leaky capacitors lose a brownish crystalline mass, which has not been analysed so far (see Fig. 1). The thermogravimetric analysis of a 1-M $[(C_2H_5)_4N]BF_4$ solution in acetonitrile showed that supercapacitors can temporarily be operated at temperatures of up to 100 °C due to the ebullioscopic effect [7]. Unfortunately, an increasing pressure is built up inside the capacitor by excess acetonitrile, desorbing inert gases, water vapor and decomposition products.

Kötz and co-workers [5] detected CO_2, propene, and H_2 in the gas space above a double-layer capacitor cell made of activated carbon electrodes and a solution of tetraethylammonium-tetrafluoroborate in propylene carbonate (PC). The major part of propene was evolved at cell voltages above 2.6 V, whereas CO_2 (mass 44) was released rather slowly at lower voltages.

Earlier observations [7] stressed the serious role of water in the electroactive materials of a supercapacitor. Ten parts per million (0.001%) water dissolved in the electrolyte lessen the

Fig. 1. Salt deposits U on the case of a burst ultracapacitor after extended operation at high temperatures and abusive voltages.

voltage window by about 10 mV compared with the dry electrolyte. Moreover, commercial carbon electrodes absorb water which cannot be completely removed even by drying at temperatures up to 150 °C.

Based on our initial assumption that acetamide and organic acids could be formed in supercapacitors, we tried to gather the first fundamental insights into the decomposition of acetonitrile electrolytes by help of spectroscopic, thermoanalytical, chemical and electrochemical methods.

2. Experimental

Our investigations try to answer the following questions:

(1) Which solid, liquid and gaseous decomposition products occur at high temperatures and abusive operating voltages?
(2) What are the precursors of the deposits on the electrode materials, in the bulk electrolyte and in the gas phase above the electrolyte?
(3) Which chemical reactions and phase changes dominate the aging processes?
(4) Which components of commercial supercapacitors cause the aging phenomena?
(5) Which conclusions about the long-term stability of supercapacitors can be drawn?

We employed comparative tests in fresh and aged electrolyte samples, consisting of a 1-M solution of tetraethylammonium-tetrafluoroborate in acetonitrile (Honeywell "Digirena E"). We used acetonitrile p.a. (≤50 ppm water), and $[(C_2H_5)_4N]BF_4$ from Merck, activated carbon electrodes on aluminium support from W.L. Gore, commercial capacitors from Epcos (Ultracap 2700 F) and Maxwell (type BCAP0350).

2.1. Sample preparation

Ten millilitres headspace vials with screwtop and PTFE/butyl rubber septa were filled with (a) about 4 ml pure electrolyte and (b) electrolyte in contact with about 20 cm² of electrode material. Moisture and air were excluded by handling the samples under a stream of nitrogen in an exsiccator. The samples were aged at room temperature and in a drying oven at 70 °C for more than 500 h. Additionally, samples were prepared in air and small amounts of water were added.

2.2. Electrolysis

Fifty millilitres of ready-made electrolyte in a beaker between two active carbon electrodes (area 28 cm², distance 3 cm) were electrolysed (a) at 6 V for 2.5 h and (b) at 4 V for 30 h in air and using a power supply (Gossen "Konstanter" SSP). The crystalline deposits on anode and cathode, and in the residual electrolyte were investigated intensively. Evaporated acetonitrile was filled up in the 4 V experiment only.

To investigate the effect of air, electrolysis was repeated in a 250 ml gas-tight bottle, which was flooded by nitrogen (see Fig. 2). The absorption vial inside was filled with pure acetonitrile to absorb gaseous decomposition products.

2.3. GC–MS

One hundred microlitres of the volatile organic compounds in headspace vials were injected by help of a gas-tight syringe into a Perkin-Elmer "Autosystem" chromatograph, coupled with a "Qmass" mass spectrometer. The liquid phase (5 μl) was injected directly by a microlitre syringe. The mobile phase was
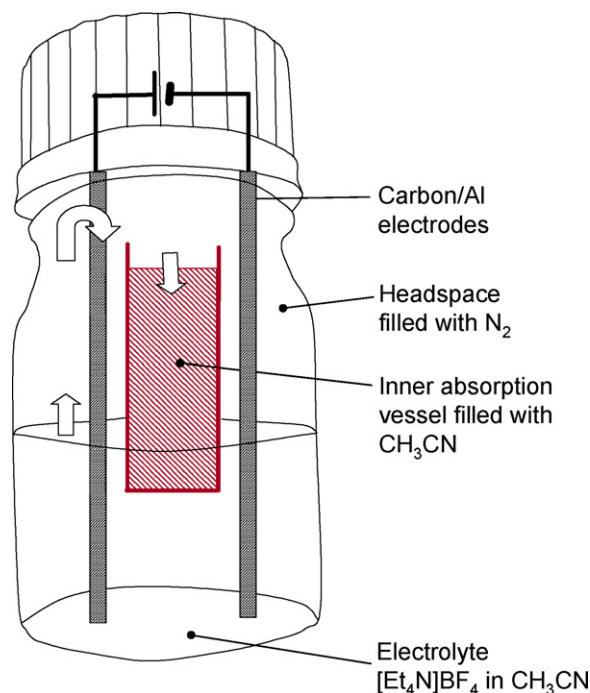

Fig. 2. Reaction bottle for aging tests at 70 °C. The screw-cap contains a polymer septum to allow headspace GC–MS analysis.

helium (45 kPa). The temperature ramp was from 50 to 280 °C at 10 K min^{-1}. Organic acids were additionally determined using a GC–FID system. Aged supercapacitors were tapped on by a steel cannula or a silicon septum was provided in the hermetically closed aluminium case.

2.4. Thermogravimetric analysis (TGA)

Using a Perkin-Elmer "Gravimetric Analyzer TGA 6", we investigated pure acetonitrile, the finished electrolyte, and the subliming and crystalline products at anode and cathode after electrolysis.

2.5. X-ray diffraction

The salt residues at burst supercapacitors were investigated by a Bruker XRD system.

2.6. IR spectroscopy

Liquids and solids were measured on a ATR unit in a FTIR spectrometer (Perkin-Elmer "Spectrum BX").

2.7. UV–vis

Acetamide was identified using UV–vis spectroscopy [8] (Perkin-Elmer "Lambda 20"). We were not able to determine NH$_4$–N directly in [(C$_2$H$_5$)$_4$N]BF$_4$/acetonitrile solutions by the indophenol method in a spectralphotometer (Dr. Lange). The Kjeldahl method was not applied.

2.8. Chemical tests

pH values were measured using a glass electrode (Metrohm "Solvotrode") and indicator strips (Baker-pHIX). Fluoride and borate were identified in 1 ml liquid sample by precipitation with eight drops of AgNO$_3$ or CaCl$_2$·2H$_2$O (10% in water), respectively. All the tests were verified by adding 0.1 ml of 10% solutions of NaF and NaBO$_2$. In a blank test, the [(C$_2$H$_5$)$_4$N]BF$_4$/acetonitrile electrolyte did not show any reactions with silver and calcium ions.

2.9. Turbidimetry

We identified tetrafluoroborate by help of the turbidness caused by the precipitation reaction K$^+$ + BF$_4^-$ → KBF$_4$ in a spectralphotometer at 780 nm. By diluting of the finished electrolyte with water and adding 10% aqueous KCl solution, we could verify a nonlinear calibration curve of absorbance versus the BF$_4^-$ concentration: $A = -0.0038 + 0.055c - 7.80 \times 10^{-4}c + 3.99 \times 10^{-6}c^3$ (fit quality 99.95%), whereby $c = 1$ corresponds to the saturated solution containing 22% of [(C$_2$H$_5$)$_4$N]BF$_4$ in acetonitrile.

2.10. TOF-SIMS

The electrodes in contact with the electrolyte were investigated by secondary ion mass spectrometry using Ar$^+$ (10 keV) as primary ion. The mass resolution was better than 5000.

3. Results and discussion

3.1. Salt residues in burst supercapacitors

By help of X-ray diffraction, IR and UV–vis spectra, and TGA, we investigated the brownish salt residues on the case of the ultracapacitor in Fig. 1, which failed after a long time of operation at high voltages. The unexpected variety of compounds in this crystalline mass is partly due to several weeks of storing in ambient air. Besides the decomposition products of [(C$_2$H$_5$)$_4$N]BF$_4$, the evaluation of the XRD spectrum in Fig. 3
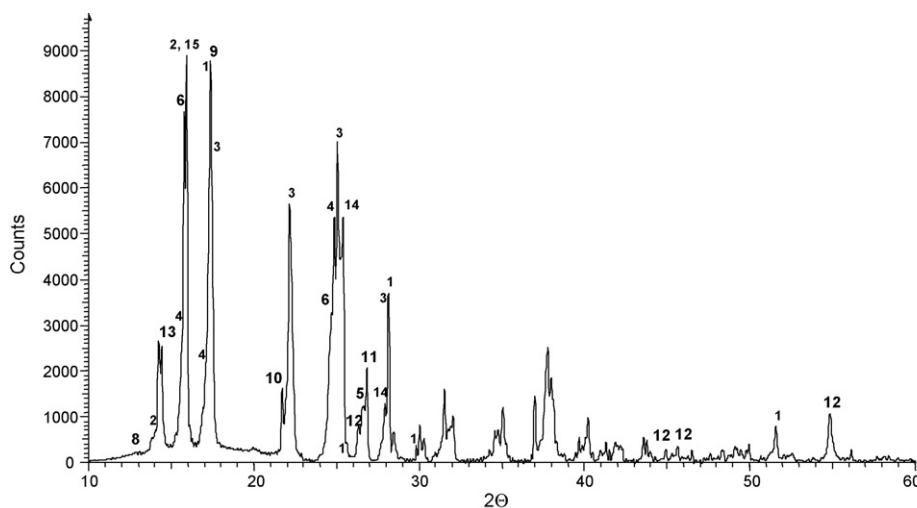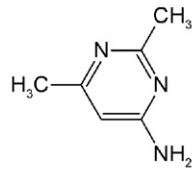

Fig. 3. X-ray diffractogram (XRD) of the salt residue *U* on the supercapacitor in Fig. 1. (1) (NR$_4$)$_4$BF$_4$, (2) 1-adamantanol, (3) maleic acid, (4) hexahydroanthracene, (5) dimethylglyoxime, (6) 2-fluorophenoxyacetic acid, (7) norgestrel C$_{21}$H$_{28}$O$_2$, (8) 1,4-naphthoquinone, (9) *p*-toluic acid, (10) poly(1,3-propanediol), (11) acetamide, (12) carbon, (13) quinolinic acid, (14) terephthalic acid, (15) 1-methylthymine, (16) 2-tertbutyl-anthraquinone, and (17) *p*-glyoxyl-anisidine-acetyl-oxime. [7, 16, 17 are superimposed by other peaks.]

Table 1
Plausible reactions of acetonitrile and its oxidation products which are consistent to the analytical findings

gives hints at acetamide, aromatic and unsaturated organic acids, derivates of fluoroacetic acid, oximes, and macromolecular compounds.

Acetamide and its derivates occur as the direct and indirect decompositions products of acetonitrile. In contact to traces of water, the hydrolysis of amides ends at organic acids, which is well known from organic chemistry according to reaction (1) in Table 1. Derivates of fluoroacetic acid illuminate a different reaction route by hydrohalogenation (2), in which aromatic hydrocarbons steming from the carbon electrodes can take part obviously. Aromatic hydrocarbons, carboxylic acids, and quinones cannot be found in thermally aged electrolyte samples, but they were detected if a piece of activated carbon electrode was present during aging the electrolyte (see Section 3.6 about catalytical effects). Traces of oximes, which were detected both by XRD and IR spectroscopy, might be the precursors of a Beckmann rearrangement to lactames and polyamides.

The XRD results, indicating the presence of amides, were verified by thermal analysis and IR spectroscopy. In Fig. 4a, solid acetamide shows its strong IR absorption bands of the asymmetric and symmetric valence vibrations at ~3350 and 3180 cm^{-1}, respectively. ν(CO) occurs at 1660, ν(CN) at 1390, δ(NH$_2$) at 1615, 1150 (rocking) and ~700 cm^{-1} (wagging). The IR spectra of the brownish residues on the burst capacitor U and the anodic deposit A after electrolysis at 4 V are quite similar, as shown in Fig. 4b. Tiny shoulders at ~1700, 1636 and 1435 cm^{-1} indicate unsaturated organic acids, although they are covered by stronger bands. Obviously, a small portion of acetonitrile is able to dimerisate and to form maleic acid by hydrolysis. The quite similar cathodic conversion of acrylonitrile to adiponitrile is well known in organic electrosynthesis (see Table 1).

3.2. Accelerated aging by electrolysis

With respect to the aging mechanisms, we were able to reproduce a similar crystalline mass as in the burst ultracapacitor in Fig. 1 by electrolysis of acetonitrile/[(C$_2$H$_5$)$_4$N]BF$_4$ electrolyte between two activated carbon/aluminium electrodes (purchased from Gore), in a distance of about 3 cm.
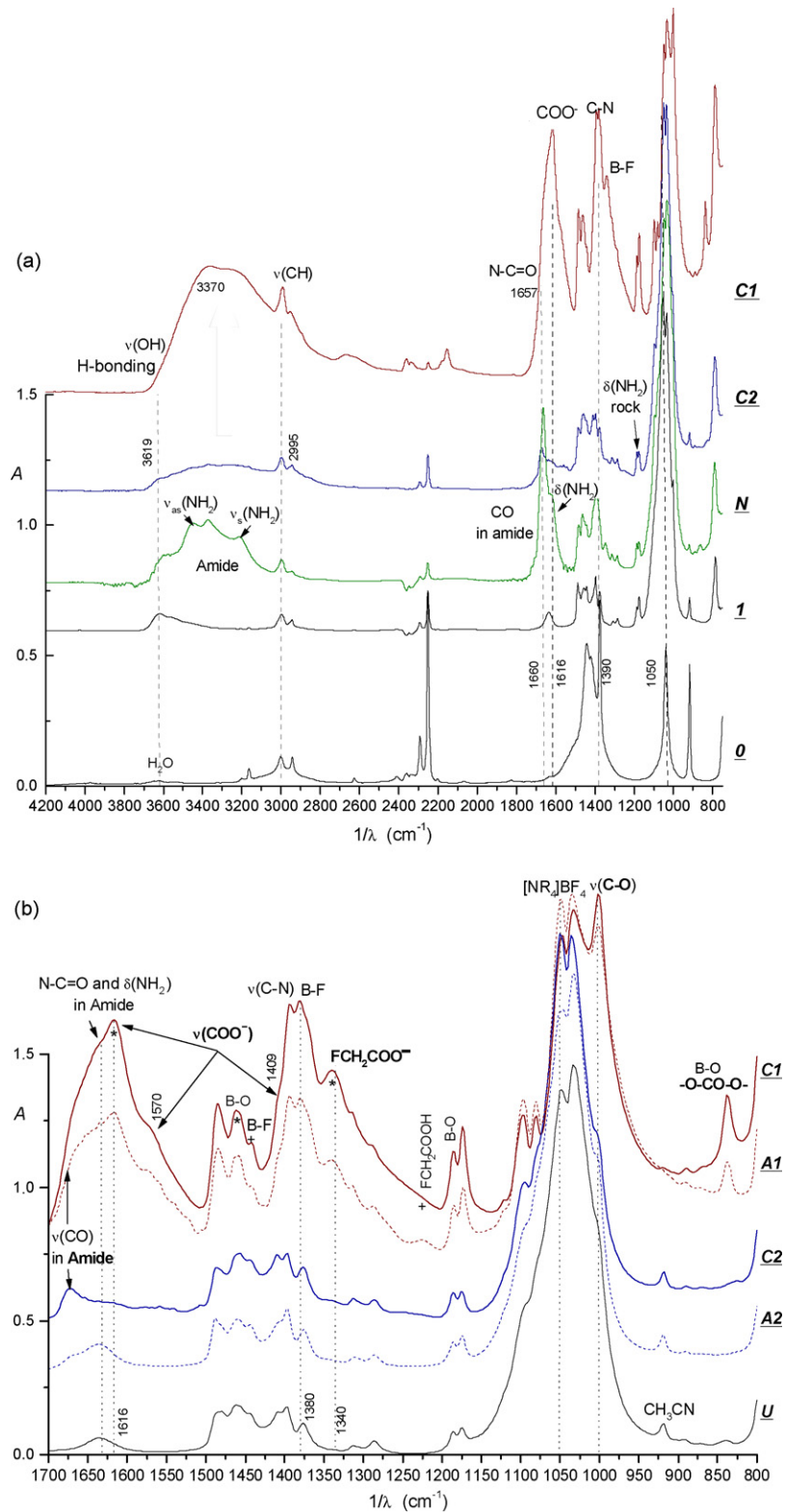
Fig. 4. (a) FTIR spectra of the deposit *C* on active carbon cathodes after electrolysis in [(C₂H₅)₄N]BF₄/acetonitrile solution ((1) 6 V, 2.5 h; (2) 4 V, 30 h), in comparison to acetamide *N*, fresh electrolyte *1* and pure acetonitrile *0*. (b) IR bands which indicate the formation of amides and fluorocarboxylate. Comparison of the electrolytic deposits at the cathode *C* and anode *A* ((1) 6 V, 2.5 h; (2) 4 V, 30 h) and the crystals on the burst ultracapacitor *U*. (c) FTIR band assigned to the ionic interactions of BF₄⁻ and alkylammonium ions (structure) in the electrolyte *1*; after precipitation with potassium chloride; and in electrolytic deposit *C1* (6 V, 15 h, after 4 days in air).
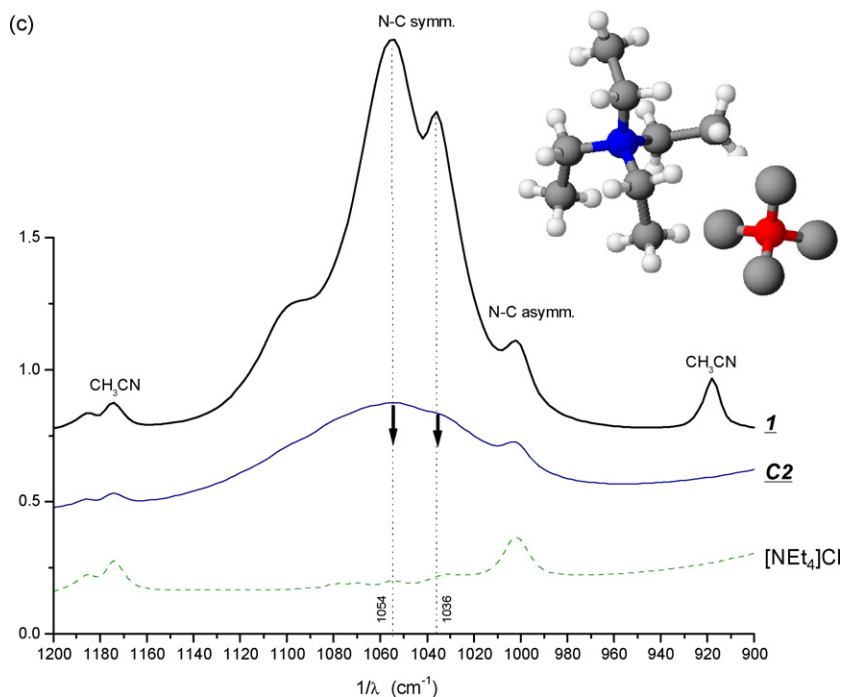
Fig. 4. (*Continued*).

(a) Right from the start of the 6 V electrolysis, we observed the formation of gas bubbles at both electrodes and the generation of brown products which are soluble in acetonitrile and crystallize on the cathode surface (negative pole). The decomposition is acompanied by the white smoke of a sublimating microcrystalline fraction. At the anode (positive pole) a white deposit precipitates. The pH in the dark brown, liquid phase changes from alkaline to acid during electrolysis. In the residual electrolyte we could identify fluoride and borates by precipitation with calcium and silver ions (method see Section 2). Obviously hydrogenfluoride is formed.

The white and brown crystals burn with a green flame (such as boric acid alkyl esters do) while alkaline gases escape—just in the same way as acetamide and ammonium acetate behave. $[(C_2H_5)_4N]BF_4$ crystals burn releasing first acidic and then alkaline gases. The evolution of acidic and alkaline gases was identified qualitatively by pH strips; a GC–MS analysis reveals the presence of HF and amines (see below).

(b) At a lower decomposition voltage of 4 V, considerable gas formation was not observed. In the course of time, light brown products appeared in the electrolyte, which were not soluble both in acetonitrile and in water. Contrariwise, the deposits on cathode and anode are well soluble, except for a small amount of dark brown products.

The IR spectra of the anode and cathode films in Fig. 4a and b give clear hints at the formation of intermediate amides (3200–3400, $\sim$1640 cm^{-1}) and carboxylate anions of organic acids ($\sim$1570, $\sim$1430, $\sim$1100 cm^{-1}). The valence vibration at 1051 cm^{-1} is found in ammonium acetate, too. Acetonitrile absorbs in a different spectral range ($\sim$3000, 2293/2246,

1442/1375, 1040, 917, and 748 cm^{-1}). The 1174 cm^{-1} band occurs in the fresh and aged electrolyte—a typical sign for secondary amines which stem from $[N(CH_2CH_3)_2]^+$ ions. One thousand six hundred and seventy-two per centimetres is also found in *N*-alkylamines. The IR doublet at 3550–3300 cm^{-1} can possibly be assigned to *enamines* such as 3-aminobut-2-ene nitrile, which is generated by dimerisation of acetonitrile according to reaction (3) in Table 1.

The thermogravimetric curves of the electrolytic deposits in Fig. 5 exhibit a step at 225 °C which can reproduced by the decomposition of additive acetamide. The main step at 495 °C is due to the decomposition of the electrolyte, mainly the alkylammonium ion followed by the more stable tetrafluoroborate. Acetonitrile evaporates far earlier below 140 °C. The TGA curves of the active carbon electrode shows a linear decay
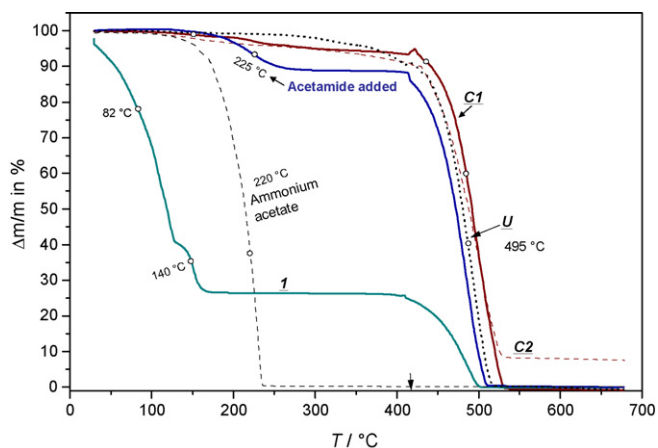

Fig. 5. TGA curves of the electrolytes deposits *C1* (6 V, 2.5 h), *C2* (4 V, 30 h) on active carbon cathodes in $[(C_2H_5)_4N]BF_4$/acetonitrile *1* in comparison with the bloom on the burst ultracapacitor *U*.

up to 450 °C due to desorbing water, followed by two steps at 620 and 840 °C. The transition at 620 °C is also found in the anodic residue of the electrolysis experiment. We conclude that the active carbon material is mainly destroyed at the anode.

In the headspace GC–MS analysis of the electrolysis experiment we found the masses 41 (acetonitrile), 29 (ethyl), 20 (HF) and hints at complicated products. In the liquid phase, with a plausibility of 55%, we found 1,1′,1″-nitrilotris-1-propanol, the oxidation product of *triethylamine*, in which the ethyl branches carry additional OH groups. The subsequent acid was detected as its ethyl ester $N(CH_2COOCH_2CH_3)_3$ by a plausibility of 36%.

In the solid residue on the cathode, which was solved in acetonitrile, we identified *heterocyclic compounds* and fluorinated aromatic hydrocarbons. Certainly, further investigations must be conducted to clarify these exotic reaction products, which are generated by the electrolysis of acetonitrile/$N(CH_2CH_3)_4BF_4$ at carbon electrodes at cell voltages above 4–6 V, whether or not air is present. Good compliance to reference spectra in the NIST database were given for 2,6-dimethyl-4-pyrimidinamine and N,2-dimethylpropanamide. Surprisingly, mass 44 ($C_2H_6N^+$) gives evidence for 1-Adamantanemethylamine with a plausibility of 76%, which is confirmed by the XRD results. It is known in organic chemistry [9] that perhydro-dicyclopentadiene forms adamantan in presence of Lewis acids. Dicyclopentadiene alcohols and ketones are widely used as solvents and for the production of plasticisers, lubricating oils and polyesters. We have no doubt that these components might be contained in commercial supercapacitors.

We conclude that the salt residues on burst supercapacitors, containing acetamide, organic acids and heterocyclic compounds, can be reproduced by electrolysis at cell voltages above 4–6 V.

3.3. Organic acids

By help of GC–FID, 0.2–0.6% of *acetic acid* were detected in the acidified deposits on the active carbon anode. Free linear carboxylic acids higher than acetic acid play no role. In the cathodic residues, organic acid could not be detected at all. About 1.5% of acetic acid was found in the insoluble residue of the 4 V electrolysis. We conclude that acetic acid seems to be generated by the hydrolysis of acetonitrile and its precursor acetamide. In alkaline solution ammonium acetate is formed according to reaction (1) in Table 1. But what happens in a completely dry system? Can fluorine play the role of water?

We observed the formation *fluoroacetic acid* derivates in the anodic and the cathodic residues of electrolysis at a cell voltage of 6 V. Interestingly, 4 V were not enough! This is consistent to the fact, that the electrochemical fluorination of carboxylic acids in hydrogenfluoride by the Simons' process [9] requires cell voltages of 5–8 V (reaction (7) in Table 1).

In Fig. 4b, the IR spectra of the anodic and cathodic residues show peaks at 1340 and 1616 cm^{-1}, typical of fluoroacetate, which disappears after several weeks of storing at ambient air. Spectral data of pure fluoroacetate show the same peaks. The IR bands of free fluoroacetic acid appear far less intensively at 1438 and 1213 cm^{-1} [10]. Fluoroacetic acid melts at 35 °C and

boils at 165 °C. The thermogravimetric curves show a shoulder at 151 °C during the decomposition of the acidified residues, which is also present in [$(C_2H_5)_4N$]BF_4/acetonitrile electrolyte, but is missing in pure acetonitrile and pure salt.

Furthermore, chemical observations indicate the formation of *hydrogenfluoride*. Heating crystallic samples in glass vials, the characteristic oily gas bubbles creep up the etched glass walls. The ceramic crucible and the metallic lid of our thermogravimetric analyser were attacked aggressively.

We conclude that the decomposition of acetonitrile in TEABF$_4$ at cell voltages of about 6 V leads to fluoroacetic acid and a wealth of conversion products.

3.4. Aromatics in the UV spectra

Pure acetonitrile, and the electrolyte solution do not absorb UV–vis light below 800 nm. After 10 h of electrolysis in a gastight vessel, flooded with nitrogen, however, marked absorption peaks arise in the samples of the decomposed electrolyte. The deposits on the active carbon electrodes and the crystals U on the burst ultracapacitor, dissolved in acetonitrile, show similar UV–vis spectra (Fig. 7). The strong peak at 220 nm is also found in acetamide and was assigned to the $n \rightarrow \pi*$ transition of electrons in the CO group [11]. Organic acids show a band in the same region, but at somewhat lower wavelength. The absorption peak at 260 nm is typical of the chromophoric group CN=N, and the $\pi \rightarrow \pi*$ transition in aromatic double bonds [12]. We state evidence for organic acids, amides, and volatile aromatic compounds.

The gases formed during electrolysis were absorbed in an inner vessel filled with acetonitrile as shown in Fig. 2. The pH in it changed to acidic (pH 5), whereby fluoride could not be detected by a precipitation reaction with calcium ions. pH 7 was measured before in the pure electrolyte by indicator strips and a glass electrode, although in this non-aqueous electrolyte the true neutral point might be slightly different from pH 7.

3.5. Colored and polymer products

The brown deposits on the electrodes and on the burst ultracapacitor, existing after electrolysis only, led us to the analogy of the Maillard reaction [13] according to reaction (6) in Table 1. Indeed, we found *pyrazine* structures in the liquid and gaseous phase of our closed model reactor (Fig. 2). The stable pyrazine ring is generated by condensation of two α-amino-carbonyl compounds. The substituents at the pyrazine ring, we were able to detect by GC–MS, were alkyl rests and CN-groups. GC–MS spectra not shown here give hints at piperidine, pyrimidine and indol derivates, which were connected to fluoroaromates and N,N-dialkylamides, respectively.

A certain portion of the electrolytic decomposition products C at 4 and 6 V is not soluble in acetonitrile, contains active carbon particles, attracts water, and the taste of acetic acid is perceptible, when it is dried at air. With respect to the polymer-like characteristics, we assume the formation of *polyamides* during electrolysis. In the IR spectra, not shown here, the shoulder at 3050 cm^{-1}, and the IR bands at 1650 and 1560 cm^{-1}, related
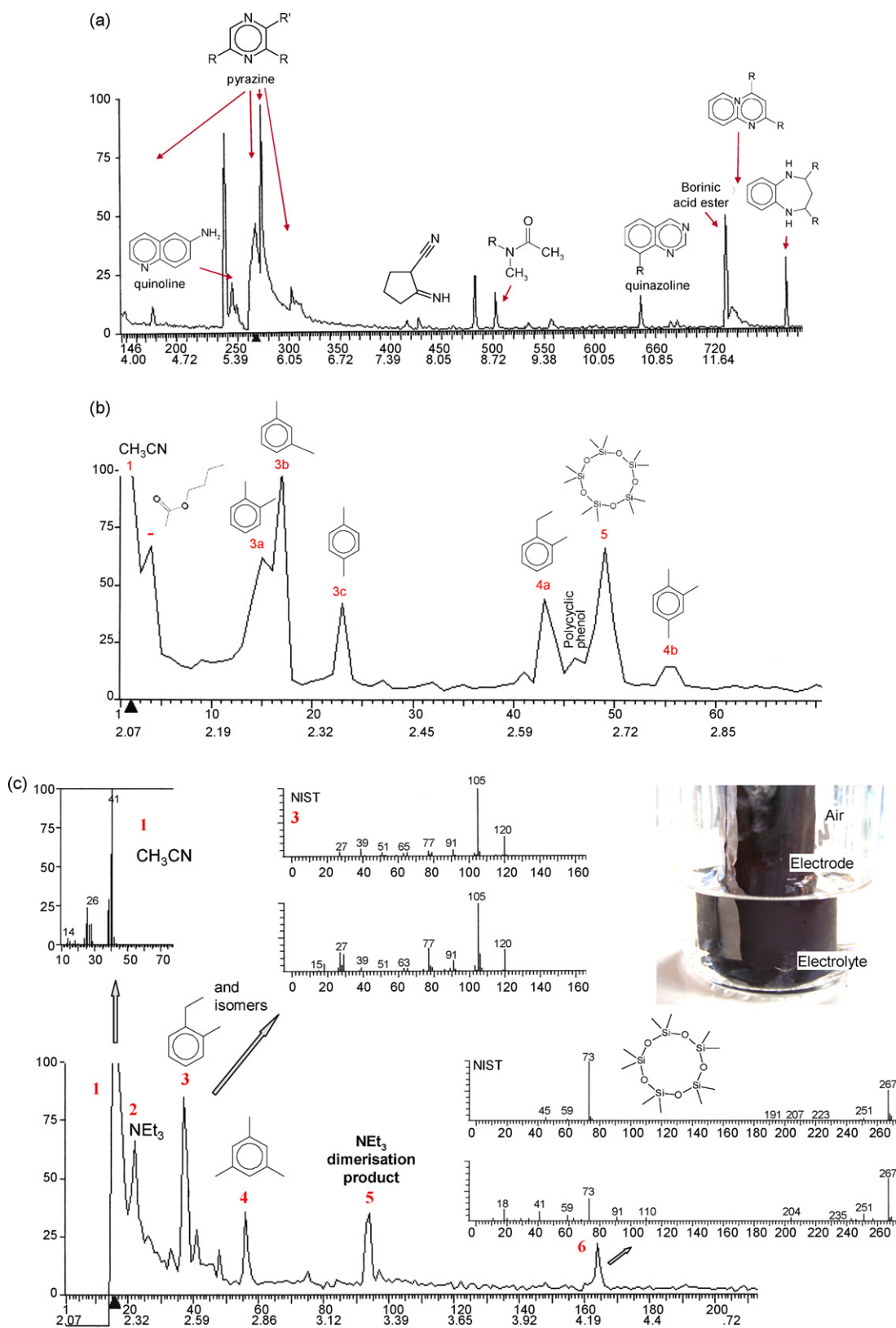
Fig. 6. (a) GC–MS analysis (70–280 °C at 10 °C min^{-1}) of the electrolysis products in the liquid [(C$_2$H$_5$)$_4$N]BF$_4$/acetonitrile phase (6 V, 2.5 h, N$_2$, see Fig. 2). (b) GC–MS analysis of the thermal decomposition products in pure acetonitrile. Contaminations in the active carbon/aluminium electrode (70 °C, 550 h). (c) Thermal decomposition of TEABF$_4$/acetonitrile in presence of an active carbon electrode (70 °C, 550 h). (d) Decomposition products in the headspace of a supercapacitor aged at 2.5 V (70 °C, 1000 h). 42–44: C$_2$H$_4$N$^+$–C$_2$H$_6$N$^+$, 56–58: C$_3$H$_6$N$^+$–C$_3$H$_8$N$^+$.

Fig. 6. (*Continued*).

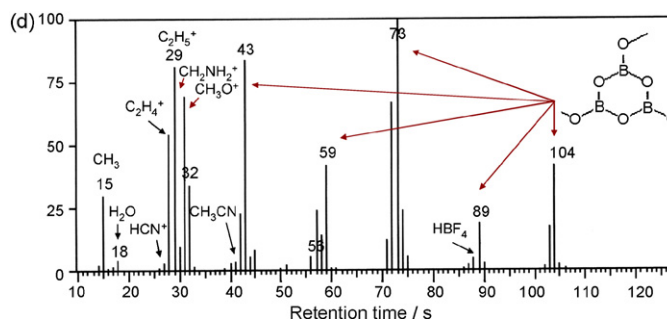to NH-vibrations, could indicate polyamides (superimposed by water at 3265 and 1635 cm^{-1}). Carboxylate bands, such as in ammonium acetate, appear at different wave numbers (1570, 1410 cm^{-1}).

3.6. Thermal aging: influence of active carbon

Pure acetonitrile, and TEABF$_4$/acetonitrile electrolyte were aged in headspace vials with and without contact to active carbon/aluminium electrodes and air. After more than 500 h of aging at 70 °C, we injected 5 µl of the liquid phases into the GC–MS.

We did not find any significant contaminations in the aged acetonitrile besides some butanenitrile. In the electrolyte sample, we detected negligible concentrations of fluorinated products similar to *N,N*-difluoro-2,3-butanediimine. Traces of hydrogen fluoride (mass 20) were detected both in the pure and in the aged electrolyte.

In acetonitrile (Fig. 6b) and finished electrolyte (Fig. 6c), which were in contact to the electrode material, however, we found significant amounts of *alkyl substituted aromatics*, and cyclic siloxanes, which are dissolved from the electrode material already at room temperature. Moreover, we found acetic acid butylester in aged acetonitrile.

Triethylamine and *N*-alkyl-ethanediamine could be detected only in the electrolyte aged at 70 °C.

We conclude that the thermal decomposition of the TEABF$_4$ electrolyte requires the catalytic activity of the electrode material. Pure acetonitrile behaves thermally stable. The most interesting formation of heterocyclic structures in the liquid phase requires an electrolytic current flow.

Where can siloxanes stem form? Commercial electrodes may contain silica compounds to bond the active material onto the current collector. Moreover impurities of silicon are contained in any carboneous material. In US Patent 4,605,989 is was even suggested to add 1% of SiO$_2$ to reduce the leakage current of carbon electrodes in supercapacitors.

3.7. Gaseous products

(a) In headspace vials, we identified amides, alkylamines, boranes, and heterocyclic compounds in the thermal decomposition products of [(C$_2$H$_5$)$_4$N]BF$_4$ in acetonitrile. The formation of *ethene* is indicated by mass 28 in the GC–MS.

We suppose a splitting of the quarternary ammonium salt by a Hoffmann elimination according to reaction (2) in Table 2. The byproduct triethylamine and the tertiary amine radical CH$_3$(C$_2$H$_5$)N=CH$_2^+$ (mass 72) were found, too. As a result, a proton is set free which can form HF with excess fluoride. Indeed, we found traces of HF (mass 20) in 1 µl of the electrolyte solution injected directly into the GC–MS system; oxygen and CO$_2$ (mass 44) play no role.

(b) In the gas space of supercapacitors, which were aged uncharged at 70 °C for 500 h, we found excess acetonitrile, water vapor, traces of oxygen, carbon dioxide and ethene. In a volume of 100 µl, after chromatography at 120 °C at an unpolar column, the following masses were recorded:

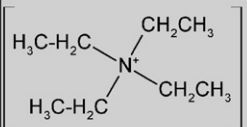- Acetonitrile: 14CH$_2^+$, 26CN$^+$, 40/41CH$_{2-3}$CN$^+$, less important: 15CH$_3^+$, 27HCN$^+$.
- Gases: 18H$_2$O$^+$, 28N$_2^+$/C$_2$H$_4^+$, 32O$_2^+$, 40Ar, 44CO$_2^+$.
- Fragments of the salt: 16NH$_2^+$, 17NH$_3^+$, 19F$^+$; traces of 20HF$^+$, 29C$_2$H$_5^+$, 30BF$^+$/CH$_2$NH$_2^+$, 39K$^+$/C$_3$H$_3^+$, 43(CH$_2$)$_2$NH$^+$/CONH$^+$, interestingly: 96CF$_3$CONH fragment.

Mass 44 plays no role in the pure electrolyte, and is thus an indicator for the presence of triethylamine, already found in the liquid phase. The difference 44C$_2$H$_6$N$^+$ → 16NH$_2^+$ corresponds to the elimination of CH$_2$=CH$_2$ due to the onium reaction of *N*-ethylamines.

The concentration of fluoride (mass 19) exceeds that of HF (mass 20). The *fluoroacetamide* fragment (mass 96) supports our IR study for the model reactor. This confirms reaction (2) in Table 1 that acetonitrile is fluorinated and forms acetamide and by hydrolysis fluoroacetic acid.

(c) In the headspace of a supercapacitor which was continuously charged at 2.5 V and 70 °C, mass 44 (from CO$_2$, besides C$_2$H$_6$N$^+$ from amine, CONH$_2^+$ from amides) and fluoride (mass 19) could be detected in significant larger amount, whereas mass 43 (from salt) dropped. Obviously, CO$_2$ and fluoride are formed as the reaction products at high currents. Mass 32 indicated that some oxygen was present in the hermetically aluminium case equipped with a septum. The oxidation of carbon and the decarboxylation of organic acids are well-known sources of CO$_2$. Dicarboxylic acids were already detected in the burst ultracapacitor by the XRD study above.

Table 2
Possible reactions of tetraethylammonium-tetrafluoroborate in acetonitrile with respect to the analytical findings

(1) Hydrolysis	$[BF_4]^-$	$[BF_4]^-$ $\rightarrow BF_3 + F^-$ $BF_3 + HF$ $\rightarrow HBF_4$ $HBF_4 + H_2O$ $\rightarrow HBF_3(OH) + HF$ $4\,BF_3 + 3\,H_2O$ $\rightarrow B(OH)_3 + 3\,HBF_4$
(2) Hoffmann elemination	(structure of tetraethylammonium ion) Y^-	$\rightarrow (C_2H_5)_3N + H_2C=CH_2 + HY$ $Y = OH^-, F^-$

3.8. Borate and fluoroboron compounds

In the headspace above the electrolyte of a supercapacitor aged at 2.5 V (70 °C, 1000 h), we identified the fragments of *metaboric acid* and alkyl boron compounds by help of the NIST database—obviously generated by the hydrolysis of BF_4 anions at elevated temperatures. It cannot completely be excluded that higher temperatures than 70 °C were reached inside the capacitor pack due to poor heat conduction. Fig. 6d shows that, the peaks of free boric acid (peak 62) und BF_3 (68) are missing. Boric acid forms metaboric acid by elimination of water at temperatures of 100–130 °C; bortrioxide is formed at 160 °C [14]. Thus we suppose that the temperatures inside a supercapacitor can easily reach more than 100 °C during the long-term operation at the specified surface temperature of 70 °C. Furthermore, the surface of the aluminium case is able to cool down effectively by thermal radiation.

The source of oxygen might be unwanted traces of water or the oxide layer of the aluminium support. Absorbed air in and above the electrode package does not fit to the small nitrogen signals (28), which superimposed by ethene additionally.

IR bands of B–O vibrations in *inorganic borates* appear at 1460 and 780 cm^{-1} [15]. The intensive combination band at 1054 cm^{-1} in Fig. 4c disappears considerably, when potassium chloride is added to the electrolyte, so that a precipitation reaction takes place: $[(C_2H_5)_4N]BF_4 + KCl \rightarrow [(C_2H_5)_4N]Cl + KBF_4\downarrow$. The comparison of IR spectra of $[(C_2H_5)_4N]Y$ with different counterions (Y=Cl, CN, Br) shows [10], that smaller counter ions allow asymmetric vibrations for account of the intensity of the symmetric coupling at 1042 cm^{-1}. The absorbance of the cathodic residues at this wave number is relatively smaller, so that the BF_4-ion seems to be stronger dissociated from the alkylammonium ion. Or it might be exchanged by different counterions, which promote the Hoffmann elimination. The B–F vibrations at 1443 and 1374 cm^{-1} should be related to the decomposition of BF_4^- ions hence (Fig. 4b). HBF_4 (mass 88) acts stronger than hydrofluoric acid, but it does not etch glass.

In the UV–vis range, we identified tetrafluoroborate by turbidimetry of the KBF_4 precipitate. Interestingly, the absorbance at 780 nm is nearly the same in the fresh electrolyte (0.1 ml contain 22 mg BF_4^-), in 22 mg of the cathodic residue of the electrolysis, and in 22 mg of the deposit of a burst ultracapacitor. The samples were diluted with acetonitrile to a volume of 2 ml and filled up with 1 ml of water. Hence, the BF_4^- ion in the electrolytes proves rather stable; considerable amounts seem not to be destroyed by electrolysis. However, we observed a hydroscopic white smoke in the gas phase above the anode, possibly evolving BF_3. BF_3 is able to catalyse Friedel–Crafts reactions, the esterification of carboxylic acids, and the polymerisation of alkenes [14]. Indeed, we found phenoxyacetic acid in the residuals of the burst ultracapacitor.

3.9. The role of water

Commercial electrolytes contain less than 10 ppm of water. Absorbed water at carbon electrodes cannot completely be removed even by drying at temperatures above 150 °C. The organic binder between carbon particles and aluminium support is destroyed before. As well, the separators, usually consisting of polyolefine, do not withstand such high temperatures. The question is whether hydrogen gas, which is formed by electrolysis of water or the Simons' process (Table 1), is able to cause a drastical increase of pressure in the capacitor.

The electrolytical generation of 1 ml hydrogen requires the electric charge of 8.6 C (2.4 mAh) and the volume of 0.8 ml water. Ten parts per million water equal about 8.5 ml in 1 l of electrolyte solution. Hence, 100 ml of electrolyte, containing
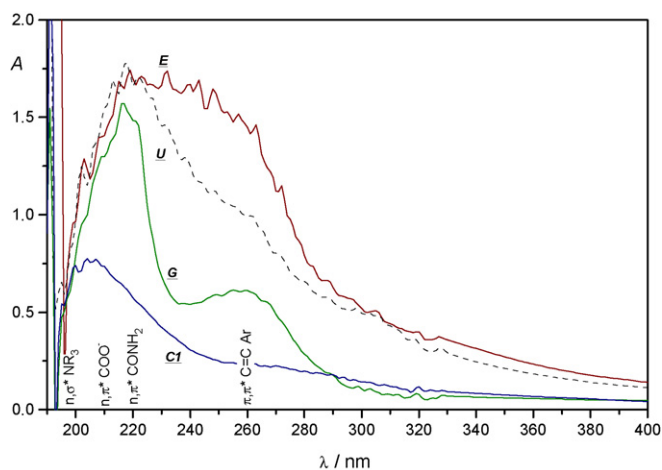

Fig. 7. UV–vis spectrum of the residual electrolyte *E* (after 6 V, 10 h, Fig. 2; 0.22% in acetonitrile), absorbed gaseous products *G*, deposit on the cathode *C1* (2.2% in acetonitrile), crystals of the burst ultracapacitor *U* (0.22% in acetonitrile).
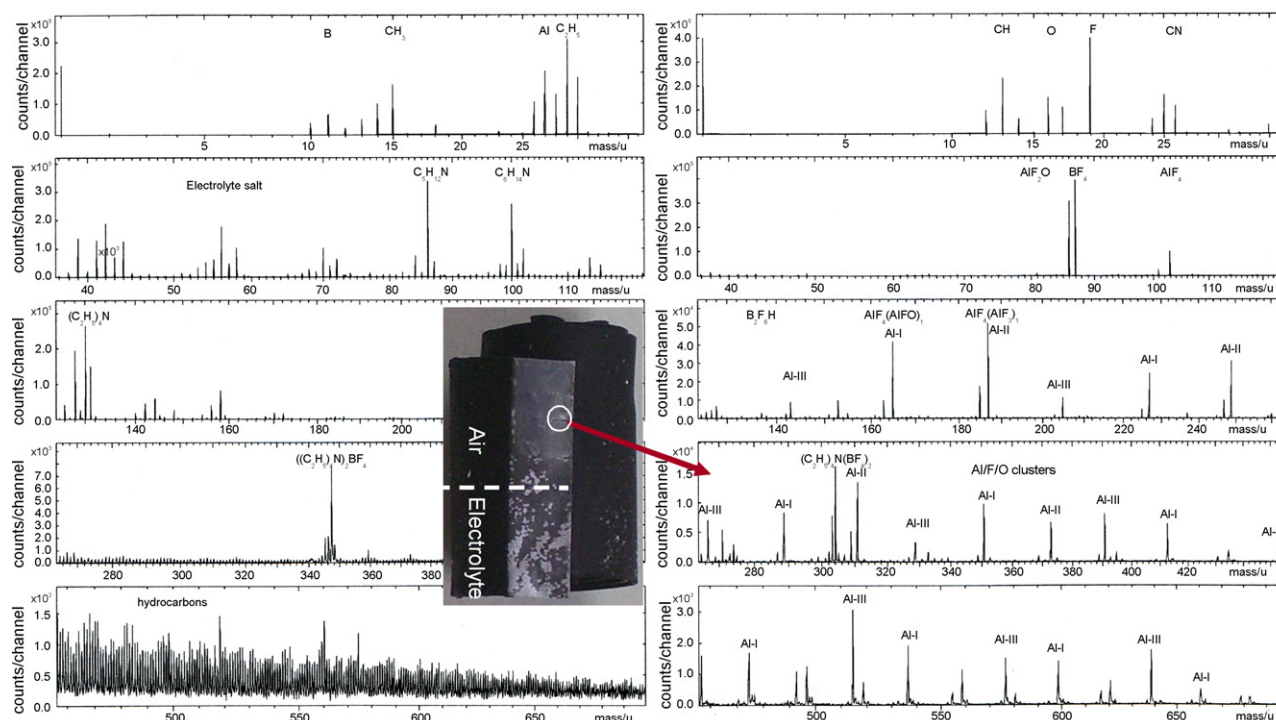
Fig. 8. TOF-SIMS spectrum of the white spots on the aluminium support below the active carbon layer after the aging in $(C_2H_5)_4NBF_4$/acetonitrile at 70 °C for 500 h. The grey aluminium support shows a nearby congruent spectrum with 10-fold lower intensities of the Al/F/O clusters.

0.85 mg water, are enough to produce about 1 ml hydrogen gas (1 mg H_2O = 1.245 ml H_2) to expand the case.

3.10. Corrosion products at the electrodes

The commercial carbon/aluminium electrode was investigated by TOF-SIMS after the thermal aging experiment in headspace vials at 70 °C for 550 h (Section 3.6). An electric voltage was not applied to the electrode. White spots appeared on the part of the aluminium foil which was immersed in the electrolyte. Aluminium which was in contact to air in the headspace showed a greyish color.

The SIMS spectrum in Fig. 8 shows deposits of $[(C_2H_5)_4N]BF_4$ and a mixture of hydrocarbons with long chains (mass 300–700) in both regions of the electrode. Besides the expected Al^+ signal, fluoroaluminate and fluorooxy aluminate complexes of the kind AlF_4^-, $AlF_4[AlOF]_n^-$ (series I), $AlF_4AlF_3(AlOF)_n^-$ (series II), and $AlF_2O(AlOF)_n^-$ (series III in Fig. 8) are present. The white spots on the part of the electrodes, which was in contact to air, show the highest intensities of the Al/F/O clusters. Signals of the kind $[Al_2O_3]_nOH^-$, which are usually found on oxidized aluminium surfaces, are completely missing. The uppermost molecular layers only are detected by SIMS.

These results let us draw the conclusion that the aluminium support underneath the carbon coating is attacked by aggressive fluoride steming from the electrolyte. It is known from literature that aluminium fluorides are more stable than fluoroboron compounds. Hence, we consider the dissolving Al_2O_3 layer on the etched aluminium support below the active carbon layer as a possible source of oxygen. Certainly, further work is necessary to understand these aging processes in supercapacitors in detail. Corrosion of the casing materials was not investigated in this study, but changes of the resistivity of electrical connections and volume changes of the spiral wound electrode package became qualitatively evident.

3.11. Ionic liquids

State-of-the-art electrolytes based on acetonitrile and propylene carbonate are limited to a potential window of about 2.5–2.7 V. On the other hand, their conductivity of about 0.1 S cm^{-1} comes close to the best inorganic electrolytes such as sulfuric acid (0.85 S cm^{-1}) and potassium hydroxide (0.62 S cm^{-1}). Recently, ionic liquids [16] have been considered as alternative organic solvents.

(a) We investigated different ionic liquids with respect to their use in supercapacitors by *ac* impedance spectroscopy [17] using a Solartron "Frequency Response Analyser 1250" in a frequency range between 10 kHz and 0.1 Hz, a sinewave excitation signal of 1 V, and a 0.1 Ω standard resistor. The measuring cell comprised two gilt copper stamps (2.5 cm × 2.5 cm) in a fixed distance of 2 mm. The vacuum capacitance of $C_0 \approx 3$ pF at 1 kHz was verified by a LCR bridge. The cell constant $K = R\kappa \approx 0.027$ cm^{-1} was determined by help of 0.1 M KCl solution ($\kappa = 0.01215$ S cm^{-1}, 22 °C) and the measured impedance real part R at 1 kHz. Capacitance at any circular frequency $\omega = 2\pi f$ was calculated from the imaginary part X of impedance with reference
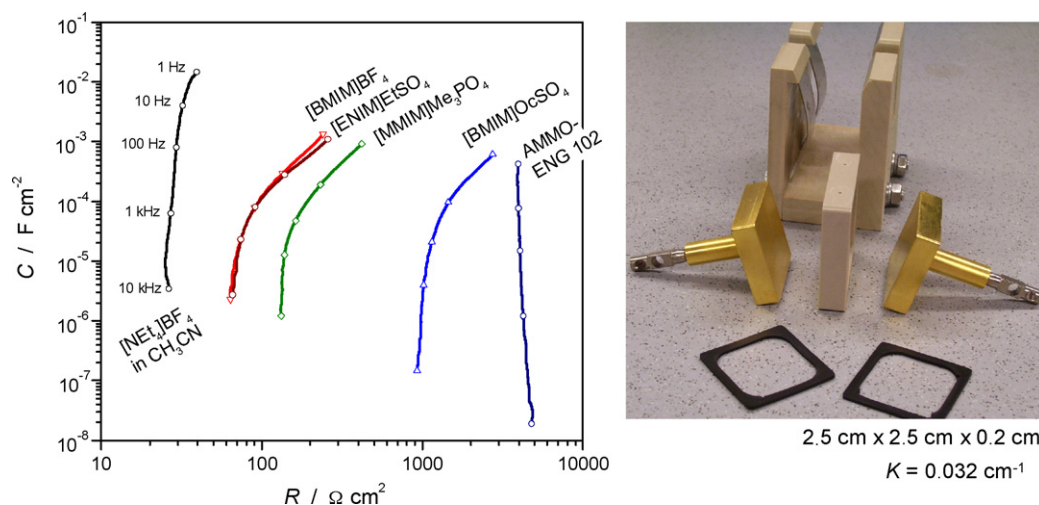
Fig. 9. *ac* impedance spectra of ionic liquids in comparison to TEABF4/acetonitrile at room temperature. Testing cell with gilt copper electrodes (right).

to a simple *R–C* series combination:

$$C(\omega) = \varepsilon K = [2\pi f X(\omega)]^{-1} \qquad (1)$$

Fig. 9 exhibits the low resistance and high capacitance of $[(C_2H_5)_4N]BF_4$ in acetonitrile in comparison to novel ionic liquids.

(b) The temperature dependence of resistance and capacitance was investigated by help of an temperature controlled glass vessel filled with 25 ml of ionic liquid, a glassy carbon working electrode, and a platinum counter electrode. This combination was chosen, because trace amounts of water and protonic impurities in the ionic liquid give rise to small reduction waves in the cyclic voltammogram on platinum but not on glassy carbon. Traces of air and moisture were allowed with respect to the technical applications. The

cell constants *K* were 0.742 (25 °C), 0.790 (40 °C), 0.850 (60 °C), 0.905 (70 °C), 1.204 (85 °C), based on literature values for the conductivity of a 1-M potassium chloride solution, $\kappa(T)$ (S cm^{-1}) = 0.00193 T (°C) + 0.0634, at a frequency of 10 kHz. Conductivity was calculated by help of the real parts of impedance according to $\kappa(\omega) = K/R(\omega)$. In all ionic liquids conductivity increased at elevated temperatures, which was to be expected for ionic conductors.

In Fig. 10, the permittivity-like quantity $\varepsilon(\omega) = 70C(\omega)/0.77$ mF was calculated as a rough estimate of dissociation and interionic forces. The measured capacitance $C(\omega)$ was divided by the capacitance of 1-M KCl solution at 0.5 Hz and multiplied by its permittivity [18], slightly decreasing at higher temperatures.

(c) Supercapacitor cells built of active carbon electrodes and ionic liquids absorbed by polymer separators did not reveal
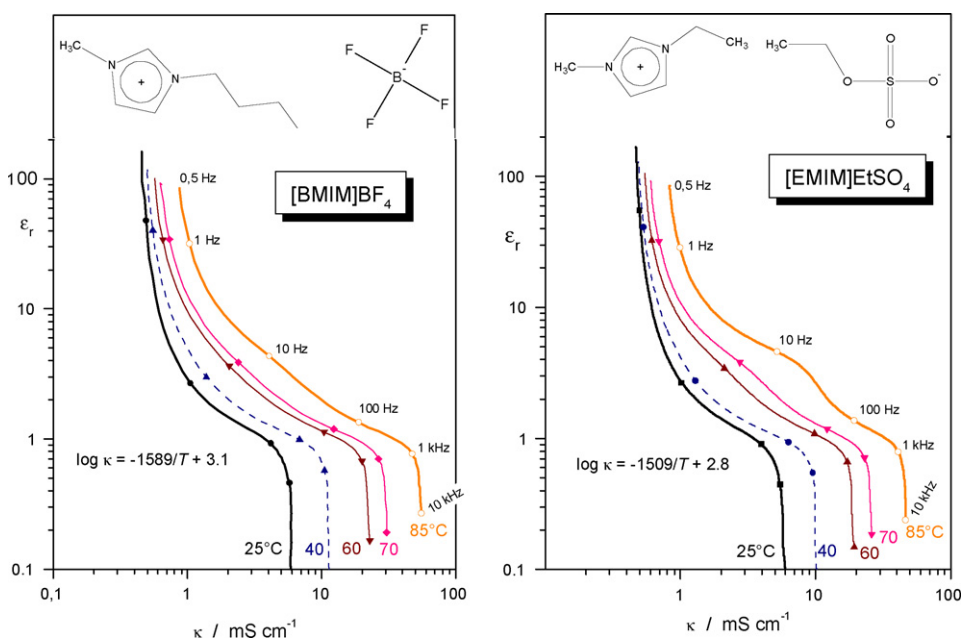

Fig. 10. Frequency response of ionc liquids at different temperatures. In the Arrhenius equation, temperature *T* is given in K.

any advantage compared to $(C_2H_5)_4NBF_4$/acetonitrile. Nevertheless, [BMIM]BF$_4$ and [EMIM]EtSO$_4$ come close. Unfortunately, the ionic liquids in the test showed an unwanted increase of leakage current due to decomposition reactions, and they tend to polymerise at cell voltages around 1.5–2 V, especially [BMIM]OcSO$_4$, AMMOENG^{TM} 102, and [MMIM]Me$_2$PO$_4$. The formation of gas bubbles, white polymer-like strings, and a brownish tinge were observed. The electrolytic and thermal decomposition was therefore not investigated in detail.

4. Conclusion and summary

We were able to gather the first insights into the thermal and electrochemical decomposition mechanisms of tetraethyl-ammonium-tetrafluoroborate in acetonitrile. Our experiments gave clear hints at the formation of volatile amines, intermediate amides, carboxylate anions of organic acids and fluorinated compounds.

(1) In the headspace of supercapacitors, excess acetonitrile, water vapor, carbon dioxide and ethene, and fragments of meta boric acid and alkylboranes were detected.

(2) The thermal decomposition of TEABF$_4$ in acetonitrile requires the catalytical activity of the active carbon electrodes.

(3) Acetonitrile forms acetamide, acetic acid and fluoroacetic acid, depending on the cell voltage and humidity of the electrolyte.

(4) The alkylammonium cation is destroyed at elevated temperatures by the elimination of ethene. The trialkylamine by-product can be oxidized. Free ammonium ions were not detected.

(5) Tetrafluoroborate is a source of fluoride, hydrogenfluoride and boric acid derivates.

(6) The brownish salt residues at burst ultracapacitors consist of acetamide, organic acids, fluoroacetic acid derivates and polymer products (polyamides?). A similar crystalline mass can be reproduced by electrolysis of the electrolyte at 4 V. The formation of fluorocarboxylic acids requires about 6 V. Acid gases escape.

(7) In the liquid phase heterocyclic compounds are formed such as pyrazines.

(8) The active carbon electrodes lose cyclic siloxanes and aromatic contaminations even at room temperature, and are destroyed mainly at the anode.

(9) The oxide layer on the etched aluminium support material under the active carbon layer is destroyed by fluorination.

(10) Hydrogen is generated by electrolysis of water and by the fluorination of carboxylic acids. Water is generated by condensation of amino-carbonyl compounds.

With respect to ionic liquids for supercapacitors, further research is required on highly conductive and chemically inert electrolytes. [BMIM]BF$_4$ might be a proper candidate to replace TEABF$_4$/acetonitrile, although its potential window is 35% more narrow.

References

[1] B.E. Conway, Electrochemical Supercapacitors, Kluwer Academic/ Plenum Publishers, 1999.
[2] W. Schmickler (Ed.), Ladungsspeicherung in der Doppelschicht, Proceeding of the 2nd Ulm Electrochemical Talks, Universitätsverlag Ulm, 1995, pp. 291–310, and literature cited there.
[3] P. Kurzweil, B. Frenzel, R. Gallay, Proceeding of the 15th International Seminar on Double Layer Capacitors, Deerfield Beach, USA, December 5–7, 2005.
[4] R. Kötz, M. Hahn, R. Gallay, J. Power Sources 154 (2006) 550–555.
[5] M. Hahn, A. Würsig, R. Gallay, P. Novák, R. Kötz, Electrochem. Commun. 7 (2005) 925–930.
[6] G. Eggert, J. Heitbaum, Electrochim. Acta 31 (1986) 1443.
[7] P. Kurzweil, H.-J. Fischle, Proceeding of the 13th International Seminar on Double Layer Capacitors, Deerfield Beach, USA, December 8–10, 2003.
[8] W. Schulz, M. Chwistek, A. Hertle, Awt Abwassertechnik 3 (1994) 6–10.
[9] Römpp Chemie Lexikon, 9th ed., G. Thieme, Stuttgart, 1995, p. 952, 1407.
[10] Merck FT-IR Atlas, Wiley–VCH, Wienheim, 1988.
[11] UV–vis Atlas of Organic Compounds, Wiley–VCH, Weinheim, 1992.
[12] Pretsch, Clerc, Seibl, Simon, Tabellen zur Strukturaufklärung Organischer Verbindungen, Spirnger, Berlin, 1981.
[13] Belitz, Grosch, Schieberle, Lehrbuch der Lebensmittelchemie, 5th ed., Springer, Berlin, 2001, p. 258ff.
[14] A.F. Holleman, E. Wiberg, Lehrbuch der Anorganischen Chemie, W. de Gruyter, Berlin, 1995, p. 1029ff.
[15] O.M. Moon, B.-C. Kang, S.-B. Lee, J.-H. Boo, Thin Solid Films 464–465 (2004) 164–169.
[16] P.C. Trulove, R.A. Mantz, in: P. Wasserscheid, T. Welton (Eds.), Ionic Liquids in Synthesis, Wiley–VCH, Weinheim, 2002.
[17] P. Kurzweil, H.-J. Fischle, J. Power Sources 127 (2004) 331–340.
[18] G. Kortüm, Lehrbuch der Elektrochemie, Verlag Chemie, Weinheim, 1970, p. 140.